Electron transfer in a covalent dye-cobalt catalyst assembly - a transient absorption spectroelectrochemistry perspective

Sebastian Bold, Linda Zedler, Ying Zhang, Julien Massin, Vincent Artero, Murielle Chavarot-Kerlidou, Benjamin Dietzek

Electron transfer in a covalent dye-cobalt catalyst assembly – a transient absorption spectroelectrochemistry perspective

Sebastian Bold,[a,b,d] Linda Zedler,[b] Ying Zhang,[a,b] Julien Massin,[d] Vincent Artero,[d] Murielle Chavarot-Kerlidou*[d] and Benjamin Dietzek*[a,b,c]

Various oxidation states of the catalytically active cobalt center in a covalent dyad were electrochemically prepared and the light-induced excited-state processes were studied. Virtually identical deactivation processes are observed, irrespective of the oxidation state of the cobalt center, varying from Co^{III} to Co^{I}, indicating the absence of oxidative quenching within the dye-catalyst assembly.

Artificial photosynthetic systems efficiently combining light-harvesting and solar energy conversion to ultimately drive multielectronic redox catalytic processes are promising candidates for solar fuels production.[1, 2] Over the last years, various molecular dyads combining a light-harvesting unit with a catalytic center (i.e. dye-catalyst dyads) were investigated, with a focus on cobalt-based assemblies for photocatalytic hydrogen production from water.[3-8] Cobalt complexes, such as the cobaloxime family, rank among the most efficient noble-metal free molecular catalysts for sunlight-driven water splitting.[9, 10] Recently, a key step was achieved with the reports of the first functional H_2-evolving photocathodes integrating such cobalt catalysts;[11, 12] in particular, we and others successfully designed fully covalent dye-catalyst assemblies combining the cobalt diimine dioxime catalyst[13] with push-pull organic dyes.[14, 15] In such dyads, an understanding of the excited state dynamics and electron transfer mechanisms is important for rationally improving the assembly design. However, they rely on a "pre-catalyst" unit where the cobalt center is in the Co^{III} state, not involved in the H_2 evolution catalytic cycle. Two successive light-driven reduction steps are thus required in order to "fully charge" the catalyst, i.e. to generate the catalytically active Co^{I} species.[13] Classical transient absorption measurements used to investigate excited state processes only allow to probe the first of these two steps, *i.e.* reduction from Co^{III} to Co^{II}, without addressing the entry point to the catalytic cycle. To overcome this limitation, we designed and built an original setup, combining the advantages of electrochemistry with transient absorption spectroscopy, to generate a specific redox state of the catalytic center as a starting point to probe relevant light-driven processes. In this study, we investigate the ultrafast excited state dynamics and intramolecular electron transfer in the photo-electrocatalytically active dyad **2**[14] using classical spectroscopic techniques (time-resolved emission and transient absorption) and, for the first time, by transient absorption spectroelectrochemistry (TA-SEC).

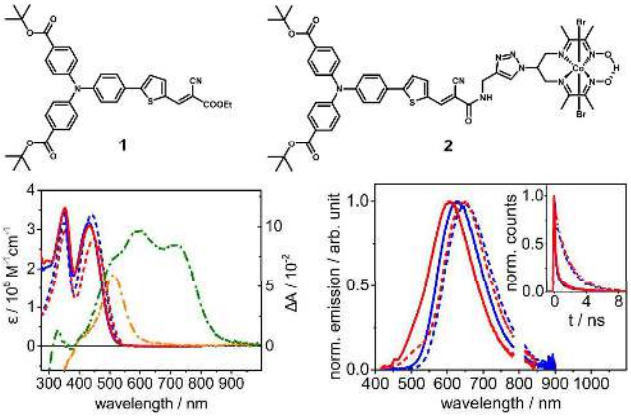

Fig. 1 Top: Structures of **1** and **2**. Bottom: UV-Vis absorption (left, ε) and normalized emission (right; λ_{exc} = 400 nm) spectra of **1** (dashed) and **2** (solid) in ACN (blue) and DMF (red). Inset in the bottom right graph: time-resolved emission of **1** and **2** in ACN and DMF. Dashed-dot lines (ΔA) in the bottom left graph: UV-Vis SEC differential spectra of **2** in DMF in the Co^{II} (orange) and Co^{I} (green) state.

Absorption spectra of the reference dye **1**[16] and of the dye-catalyst assembly **2**[14] show a peak at 350 nm, unaffected by the catalyst, assigned to a π–π* transition localized on the tri-arylamine moiety (Fig. 1).[17] At longer wavelengths, both **1** and **2** show the expected intramolecular charge transfer (ICT) transition from the triarylamine donor to the cyanoacrylate/ acrylamide acceptor moiety,[14,16] which is slightly shifted for **2**

[a] *Institute of Physical Chemistry and Abbe Center of Photonics, Friedrich Schiller University Jena, Helmholtzweg 4, 07743 Jena, Germany.*
[b] *Department Functional Interfaces, Leibniz Institute of Photonic Technology Jena (IPHT), Albert-Einstein-Straße 9, 07745 Jena, Germany.*
[c] *Center for Energy and Environmental Chemistry, Friedrich Schiller University Jena, Philosophenweg 8, 07743 Jena, Germany.*
[d] *Laboratoire de Chimie et Biologie des Métaux, Université Grenoble Alpes, CNRS, CEA, 17 rue des Martyrs, 38000 Grenoble, France.*
Electronic Supplementary Information (ESI) available: Experimental details; UV-vis absorption, time-resolved emission and transient absorption data in ACN and in DMF; UV-vis SEC and TA-SEC data in DMF. See DOI: 10.1039/x0xx00000x

in comparison to **1** (432 *vs.* 441 nm in ACN). This might be due to a weaker electron-withdrawing effect of the amide as compared to the ester. A similar blue-shift is observed for the emission band of **2**, compared to **1**. The characteristic Co^{III} absorption band is observed at 300 nm for **2**.[14] This data, together with the previously reported electrochemistry,[14] supports the absence of electronic coupling between the dye and the catalyst moieties in the ground state of the covalent dyad **2**.

Time-resolved emission spectroscopy of **1** and **2** was performed in ACN and DMF (Fig. 1), as well as after deprotection and grafting on ZrO_2 films (Fig. S1) to provide information about possible quenching processes within the dyad. ZrO_2 has a wide bandgap of 5.0 eV[18] which prevents charge injection from the dye and therefore serves as a non-quenching substrate. From a semi-logarithmic plot, it becomes apparent that the decay is monoexponential for **1** in solution, while it is biexponential for **2** (Fig. S2). On ZrO_2, a stretched exponential function was used to account for the variation in local binding environment of the grafted dye. The respective fitting functions were applied to the data and the resulting lifetimes are presented in Table S2. Emission of **1** in ACN shows the longest lifetime (τ = 1745 ps). Upon introduction of the catalyst in **2**, significant quenching is observed in both solvents and especially on ZrO_2 (τ = 45 ps). This is comparable to the value obtained by Tian and coworkers when measuring a similar dye-catalyst system on ZrO_2.[15] In solution, a faster component around 200 ps appears with a relative amplitude of 90%, while the slower component is comparable to the lifetime of **1**. The biexponential decay seems to indicate the presence of two conformers with different decay rates. The observed quenching is also reflected in the quantum yields (Table S1). On ZrO_2, the emission of **2** is quenched to a degree that determination of the quantum yield was not possible. Radiative (k_R) and non-radiative (k_{NR}) decay rates calculated from the emission quantum yield and lifetime show an increase in k_{NR} by an order of magnitude for **2** compared to **1** (Table S2), leading to a dominance of non-radiative decay. On the basis of no spectral overlap between the absorption of the Co^{III} catalyst and the dye emission, this quenching might stem from an electron transfer from the excited state of the dye to the cobalt center. Indeed, oxidative quenching of the photosensitizer is thermodynamically feasible, and Tian and coworkers have assigned such a process to intramolecular oxidative quenching of a related photosensitizer by the appended cobalt catalyst, without however any spectral evidence for the reduction of the latter.[15]

Thus, to obtain more detailed insights into the excited-state deactivation pathways in **2,** transient absorption spectroscopy was performed on **1** and **2** in ACN (Fig. S3). The TA spectra of **1** consist of a ground state bleach (GSB) at around 425 nm, matching with the steady-state absorption spectrum, and a stimulated emission (SE) band at 700 nm in agreement with the emission spectrum (maximum at 653 nm) recorded in ACN. These overlap with a broad excited state absorption (ESA) band

Table 1. Lifetimes of components (in ps) obtained *via* a global four-component fit of the TA data of **1** and **2** in ACN and in DMF under different applied potentials as well as lifetimes obtained from time-resolved emission.

	solvent	τ_1	τ_2	τ_3	τ_4	$\tau_{em,1}$	$\tau_{em,2}$
1	ACN	0.2	0.9	132	1843		1745
2	ACN	0.3	1.1	82.6	467	199	2056
	DMF, OCP	0.7	2.6	67.7	351	231	2127
	DMF, Co^{II}	0.7	2.9	57.2	290		
	DMF, Co^{I}	0.6	2.0	22.3	173		

with a maximum at around 530 nm, which explains the red-shift of the SE maximum compared to the emission spectra. The dynamics of **1** will be described in detail elsewhere,[19] and can be summarized as follows: Upon photoexcitation cooling takes place on a timescale of roughly 3 ps. Subsequently the differential absorption spectra do not change until about 50 ps after which GSB, ESA and SE decay concertedly with characteristic time constants of 132 and 1843 ps. The decay to the ground state is not complete within the experimentally accessible range of delay times. **2** shows identical behaviour in the first 3 ps in ACN as **1** (Fig. S3) which is reflected in the spectrally very similar first two components and characteristic time constants as obtained by global fitting. Compared to **1** the amplitude of the SE band is severely reduced, which is in line with the reduced emission quantum yield of **2** as discussed above. After 3 ps, there is a much more rapid decay back to the ground state with values of 67.6 and 351 ps for τ_3 and τ_4 as well as a higher amplitude for the faster component (τ_3) (Table 1, Fig. S3). Spectrally, there is no difference between the DAS of τ_3 and τ_4 of **1** and **2**. Thus, it appears that the same decay processes act in **1** and **2**, but are accelerated in **2**.

To unequivocally attribute the observed excited state decay to intramolecular electron transfer, novel spectral features associated with the reduced Co center need to be observed. UV-Vis spectroelectrochemistry was thus performed on **2** in DMF (Fig. S4) in order to provide reference spectra of the different Co oxidation states. Differential spectra taken at −0.35 V (Co^{II}) and −0.65 V (Co^{I}) vs. Ag/AgCl are shown in Fig. 1.

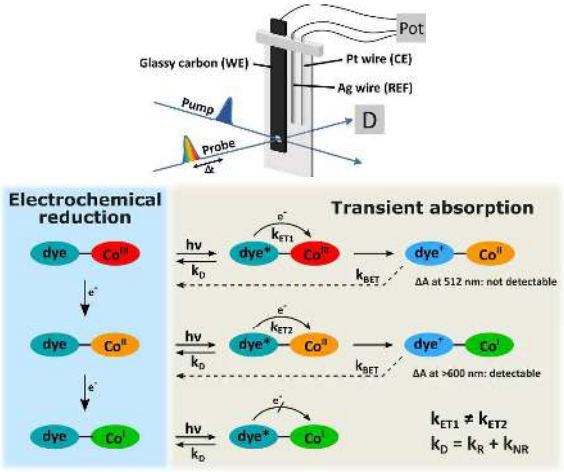

Fig. 2 Top: Schematic depiction of the cell used in the TA-SEC setup; Bottom: Scheme showing the principal reactions and processes during the TA-SEC measurement. k_D = rate of photophysical decay processes, k_{ET} = rate of electron transfer, k_{BET} = rate of back electron transfer.

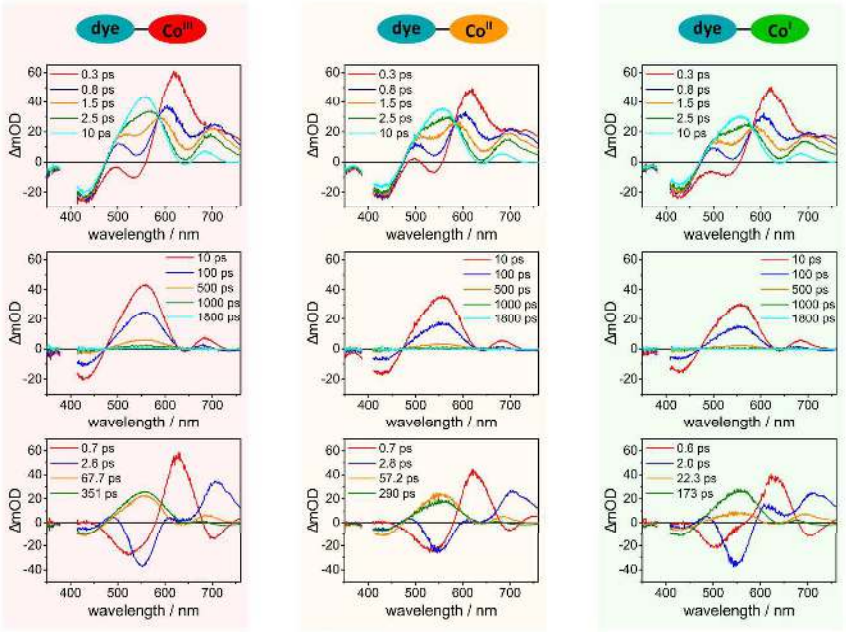

Fig. 3 TA spectra of **2** in DMF at OCP (left), at Co^{I} (middle) and at Co^{I} (right) reductive potential. The upper graphs show the spectra at early delay times while the middle ones show late delay times. The bottom graphs show the decay-associated spectra (DAS).

For the reduction to the Co^{II} state, a positive absorption band with a maximum at 512 nm arises. Upon further reduction to the Co^{I} state, a double band with maxima at 595 and 717 nm appears, in perfect agreement with the previously reported Co^{I} signature obtained for **2** during the course of a photolysis experiment.[14] Finally, reduction of the dye produces a pronounced bleach of the ICT band, which overlaps with the Co^{II} absorption band, thereby hiding it. Since the same bleach is observed for the oxidized species (Fig. S4) and as GSB in the TA measurements, it would prevent observation of the Co^{II} signature in the TA spectra if electron transfer from the excited state of the dye to the Co^{III} catalytic center occurred. However, since the Co^{I} state should be observable, a TA measurement in which the Co^{II} state is generated *in situ* by controlled potential electrolysis prior to photoexcitation, should open up the possibility of observing the occurrence of electron transfer (Fig. 2). Such a measurement would allow to study the excited state processes for **2** at the three different oxidation states of the Co catalyst, with the measurement taken at the final Co^{I} state serving as a reference since no electron transfer can occur. In summary, if intramolecular electron transfer occurs, one of the following should be observable: in case of a stable, long- lived reduced Co^{I} state, the absorption double band at 595 and 717 nm should show in the TA spectra. In case of a fast electron transfer back to the ground state, a change in the decay rate should be observed since the thermodynamic driving force for electron transfer is lower for the $Co^{II/I}$ in comparison to the $Co^{III/II}$ reduction (reduction potentials: −0.49 V vs. normal hydrogen electrode (NHE) for $Co^{III/II}$ and −0.02 V for $Co^{II/I}$ [14]). Therefore, a comparison of the excited state decay rates at different oxidation states of the Co catalyst will allow us to identify the nature of quenching observed for **2**, particularly the contribution of intramolecular electron transfer. Thus, we carried out transient absorption spectroelectrochemistry (TA-SEC) measurements (Fig. 2). First, a TA measurement at open circuit potential (OCP) was carried out to be compared against the TA measurements under an applied potential. In DMF, the spectral features of the TA spectra remain largely unchanged (Fig. 3 & S3). However, the SE band is less pronounced than in ACN (Fig. S3), correlating with the observed lower fluorescence quantum yield (0.7%), to the point where no negative signal is observed > 600 nm and the SE band is only seen as a decrease in ESA signal. The fast relaxation processes are severely slowed down in DMF such that the blue-shift of the ESA signal and build-up of the SE band are only finished within around 10 ps. At 10 ps, the TA spectrum in DMF resembles that of the 1 ps spectrum in ACN. The decrease in relaxation rates is reflected by the lifetimes obtained from the global fit for the fast relaxation processes (0.7 and 2.5 ps) which are much slower than the sub-picosecond lifetimes in ACN. This can be attributed to the higher viscosity of DMF, decelerating relaxation processes with a pronounced structural reorganization of the molecule such as rotation or flattening which have been proposed as relaxation mechanisms for this type of triphenylamine-based push-pull dye.[17] After 10 ps, an overall decay of the transient absorption spectra is observed, which reflects ground state recovery within the time window of the experiment (1800 ps). The decay rates (67.7 and 351 ps) are comparable to those obtained in ACN. TA measurements of **2** in different oxidation states of the Co-center, i.e. Co^{II} and Co^{I}, were then carried out at different applied potentials (for the CV with the applied potentials, see Fig. S5). Steady-state UV-Vis spectra recorded during the TA measurements proved the stability of the sample under measurement conditions (Fig. S5). The obtained TA spectra and DAS (Fig. 3 & S6) are strikingly similar, whatever the oxidation state of the catalytic center in **2**. In particular, the characteristic Co^{I} signature was not observed when exciting **2** at the Co^{II} state (Fig. 3 middle) so

direct spectral evidence for electron transfer from the dye to the catalyst unit was not obtained. Furthermore, comparison of the kinetic data obtained for **2** at the Co^{III} or at the Co^{II} state with the reference Co^{I} state do not provide any indirect evidence in form of markedly different decay rates. Since the kinetic rates are not notably faster in the higher Co oxidation states than in the reference Co^{I} state, electron transfer by oxidative quenching was ruled out as the emission quenching mechanism for the Co^{III} and Co^{II} states of the dyad. In fact, a counter-intuitive slightly faster decay is observed at more negative applied potentials (Table 1), contrary to expected slower ones in case of electron transfer. The acceleration of the decay at lower oxidation states might be due to coulombic repulsion of electron density on the cobalt with electron density in the LUMO of the dye located closely to the covalent linker. This would destabilize the charge transfer state and accelerate the decay to the ground state. Therefore, the data shows the absence of electron transfer from the excited dye to the catalyst in solution without a sacrificial electron donor (*e.g.*, oxidative quenching). Activation of dyad **2** thus relies on two successive electron transfers to the catalytic center from the reduced state of the dye, generated by reductive quenching of its excited state by a sacrificial electron donor (photolysis experiment) or by the photoelectrode substrate, *i.e*. NiO (H_2-evolving photocathode).[14] This also highlights that observing a quenching of emission in photoactive dyads is not always compelling proof for electron transfer and should be corroborated by using complementary techniques. Thus, the quenching of the emission lifetime for **2** compared to **1** must stem from other sources. A possible explanation for the increase in the non-radiative rate could be an increased density of vibrational modes upon adding the cobalt moiety. Also Dexter energy transfer from the excited donor chromophore to short-lived cobalt-centered dd-states might account for the observed rates at different applied potentials.

In conclusion, a dye-catalyst dyad was investigated with respect to the intramolecular photoinduced electron transfer processes. Various oxidation states of the catalytically-active cobalt center were prepared by controlled-potential electrolysis and the light-induced processes initiated by excitation of the photoactive unit were studied. We show that virtually identical photoinduced processes are observed, irrespective of the oxidation state of the cobalt center, varying from Co^{III} to Co^{I}. Thus, we conclude that oxidative quenching of the initially excited chromophore is absent in the dyad investigated and "charging of the catalyst", i.e. electron transfer from the photocenter to the cobalt center can only occur after reductive quenching of the photoactive center, *e.g*. by a sacrificial agent or by hole transfer to a NiO electrode. This is despite the shortening of the fluorescence decay time of the chromophore upon covalent attachment of the cobalt center, *i.e*. the results point to the fact that increased luminescence quenching upon introduction of a redox-active (metal) center into the molecular framework of a photosensitizer is not always unambiguous proof for electron transfer. The experimental methodology put forward here more generally allows the investigation of excited state processes, *e.g*. electron transfer but also energy transfer and structural rearrangements, in different redox states of an analyte. This is especially interesting for systems designed for multielectron catalysis where multiple electron transfer steps are needed to "fully charge" a catalyst.

Conflicts of interest

There are no conflicts to declare.

Notes and references

Acknowledgments

We thank Maria Sittig for the quantum yield data. The work was supported by the European Commission's Seventh Framework Program (FP7/2007-2013) under grant agreement n° 306398 (FP7-IDEAS-ERC, Project PhotocatH_2ode), the French National Research Agency in the framework of the "Investissements d'avenir" program (ANR-15-IDEX-02, Labex ARCANE, ANR-11-LABX-0003-01) as well as the German Science Foundation, DFG, grant No DI1517/11-1.

1. S. Berardi, S. Drouet, L. Francas, C. Gimbert-Surinach, M. Guttentag, C. Richmond, T. Stoll and A. Llobet, *Chem. Soc. Rev.*, 2014, **43**, 7501.
2. A. Thapper, S. Styring, G. Saracco, A. W. Rutherford, B. Robert, A. Magnuson, W. Lubitz, A. Llobet, P. Kurz, A. Holzwarth, S. Fiechter, H. de Groot, S. Campagna, A. Braun, H. Bercegol and V. Artero, *Green*, 2013, **3**, 43.
3. A. Fihri, V. Artero, M. Razavet, C. Baffert, W. Leibl and M. Fontecave, *Angew. Chem. Int. Ed.*, 2008, **47**, 564.
4. A. Fihri, V. Artero, A. Pereira and M. Fontecave, *Dalton Trans.*, 2008, 5567.
5. P. Zhang, M. Wang, C. Li, X. Li, J. Dong and L. Sun, *Chem. Commun.*, 2010, **46**, 8806.
6. M. Natali, R. Argazzi, C. Chiorboli, E. Iengo and F. Scandola, *Chem. Eur. J.*, 2013, **19**, 9261.
7. G.-G. Luo, K. Fang, J.-H. Wu and J. Mo, *Chem. Commun.*, 2015, **51**, 12361.
8. S. Jasimuddin, T. Yamada, K. Fukuju, J. Otsuki and K. Sakai, *Chem. Commun.*, 2010, **46**, 8466.
9. V. Artero, M. Chavarot-Kerlidou and M. Fontecave, *Angew. Chem. Int. Ed.*, 2011, **50**, 7238.
10. S. Losse, J. G. Vos and S. Rau, *Coord. Chem. Rev.*, 2010, **254**, 2492.
11. E. A. Gibson, *Chem. Soc. Rev.*, 2017, **46**, 6194.
12. V. Nikolaou, A. Charisiadis, G. Charalambidis, A. G. Coutsolelos and F. Odobel, *J. Mater. Chem. A*, 2017, **5**, 21077.
13. N. Kaeffer, M. Chavarot-Kerlidou and V. Artero, *Acc. Chem. Res.*, 2015, **48**, 1286.
14. N. Kaeffer, J. Massin, C. Lebrun, O. Renault, M. Chavarot-Kerlidou and V. Artero, *J. Am. Chem. Soc.*, 2016, **138**, 12308.
15. P. B. Pati, L. Zhang, B. Philippe, R. Fernández-Terán, S. Ahmadi, L. Tian, H. Rensmo, L. Hammarström and H. Tian, *ChemSusChem*, 2017, **10**, 2480.
16. J. Massin, M. Bräutigam, N. Kaeffer, N. Queyriaux, M. J. Field, F. H. Schacher, J. Popp, M. Chavarot-Kerlidou, B. Dietzek and V. Artero, *Interface Focus*, 2015, **5**, 20140083.
17. E. Ishow, R. Guillot, G. Buntinx and O. Poizat, *J. Photochem. Photobiol. A: Chemistry*, 2012, **234**, 27.
18. Y. Xu and M. A. A. Schoonen, *Am. Mineral.*, 2000, **85**, 543.

19. J. Massin, M. Bräutigam, M. Wächtler, S. Bold, A. B. Munoz-Garcia, M. Pavone, B. Dietzek , M. Chavarot-Kerlidou and V. Artero, Manuscript in preparation.